PERGAMON

Corrosion Science 42 (2000) 1023–1039

CORROSION SCIENCE

Activation of pure Al in an indium-containing electrolyte — an electrochemical noise and impedance study

Carmel B. Breslin*, Amy L. Rudd

Department of Chemistry, National University of Ireland Maynooth, Maynooth, Co., Kildare, Ireland

Received 20 April 1999; accepted 6 September 1999

Abstract

The activation of aluminium in an acidic indium-containing electrolyte has been studied using electrochemical noise measurements. The average pit-growth rate, measured under freely corroding conditions, was comparable in the presence and absence of indium. However, pit growth times were considerably higher in the presence of indium. The initial breakdown process followed a pseudo-first order process with a rate constant almost a factor of two greater in the case of the indium-containing solution. Analyses of the current–noise data in the frequency domain yielded spectral noise plots, which agreed well with impedance spectra measured under similar conditions. Good agreement was also obtained between R_n, which is defined as the ratio of the standard deviation in the potential noise signal to the standard deviation of the current noise signal, and the zero frequency limit of the impedance.

Keywords: Aluminium activation; Indium; Electrochemical noise data

1. Introduction

It is well known, since the pioneering work of Reding and Newport [1], that small amounts of indium, gallium, mercury and tin, when alloyed with aluminium,

* Corresponding author. Tel.: +353-1-708-36; fax: +353-1-708-3815.
E-mail address: cb.breslin@may.ie (C.B. Breslin).

0010-938X/00/$ - see front matter
PII: S0010-938X(99)00128-6

cause activation of the system [1–12]. This is characterised by a displacement of the solution potential in the electronegative direction, the ability of the system to deliver a high anodic current density, and the maintenance of an active surface that corrodes in a nearly uniform manner. Similar effects have been reported for pure aluminium in solutions containing dissolved indium salts [12].

Owing to the enhanced dissolution observed when aluminium is activated by indium in solution, this system lends itself to study by electrochemical noise analysis. Although there are some variations, this technique generally consists of measuring the current or voltage noise, or both, of two 'identical' electrodes maintained at the same potential [13–17]. Analyses of the current and potential fluctuations can then be carried out in the time and frequency domains. Analysis in the time domain involves calculation of the noise resistance, R_n, which is calculated as the ratio of the standard deviation in the voltage signal to the standard deviation in the current signal [15,18]. It has been shown, in some cases, that an inverse relationship exists between the noise resistance and the rate of corrosion [18,19].

Alternatively, power spectral density plots (PSD) of the noise can be obtained using the fast Fourier transform or maximum entropy method to transform the data into the frequency domain. The square root of the ratio of the voltage PSD to the current PSD [16,20], or the ratio of the FFTs of potential and current noise time records [21,22], sampled simultaneously, have been described as the spectral noise impedance or spectral noise response, $R_{sn}(f)$. It has been shown both experimentally and theoretically that $R_{sn}(f)$ is equivalent to the modulus of the electrochemical impedance and that $R_{sn}(f)$ is equal to R_n if $R_{sn}(f)$ is independent of frequency [20].

In this paper, the possibility of using electrochemical noise analysis to study the activation of pure aluminium in an indium-containing electrolyte is investigated. Analysis of the electrochemical noise data was carried out in both, the time and frequency domains. These data were then compared with electrochemical impedance data measured under similar conditions.

2. Experimental method

Test specimens were prepared from 99.999% aluminium obtained from Goodfellow Metals. The polycrystalline electrodes were provided in rod form and were embedded in resin, leaving an exposed surface area of 1.0 cm^2. The exposed surfaces were polished to a mirror finish using 30–0.05 micron diamond paste. They were then cleaned, ultrasonically, in methanol and dried under a stream of hot air. These electrodes, supporting a typical air-formed film, were used immediately in the corrosion tests.

An acidified 0.5 mol dm^{-3} NaCl solution, pH 1.6, and a 0.5 mol dm^{-3} NaCl solution containing 0.005 mol dm^{-3} $In_2(SO_4)_3$, pH 1.6, were used as the test solutions. Under these acidic conditions, the hydrated In^{3+} species will be predominant in the solution. The pH of the chloride solution was adjusted to 1.6

using H_2SO_4 and a sufficient amount of Na_2SO_4 (0.015 mol dm^{-3}) was added to compensate for the sulphate introduced in the indium-containing solution.

The electrochemical cell consisted of a single compartment three-electrode pyrex glass cell. In the case of the electrochemical noise data two 'identical' working electrodes were used. A saturated calomel electrode (SCE) was used as the reference electrode. It was placed equidistant between the two working electrodes, approximately 5 mm from each using a luggin probe. The electrochemical noise tests consisted of recording simultaneously the voltage and current fluctuations at a sampling rate of 2 points per second for a period of 1024 s using an ACM auto ZRA at 21°C. These data were then transformed into the frequency domain using a fast Fourier transform (FFT) algorithm.

Ac impedance data were recorded at 21°C, using an excitation voltage of 10 mV, at the corrosion potential using a Solartron 1250 FRA and 1287 potentiostat. In these tests, a three-electrode set-up was used, using high-density graphite rods as the auxiliary electrodes. The cell was undivided, but there was no evidence of any contamination of the working electrode by the auxiliary electrode reactions. A saturated calomel electrode was used as the reference electrode and was placed within a few mm of the working electrode surface using a luggin probe.

Scanning electron microscopy (SEM) coupled with energy dispersive X-ray analysis (EDAX) was used to study the surface morphology of the corroded specimens and for qualitative analyses.

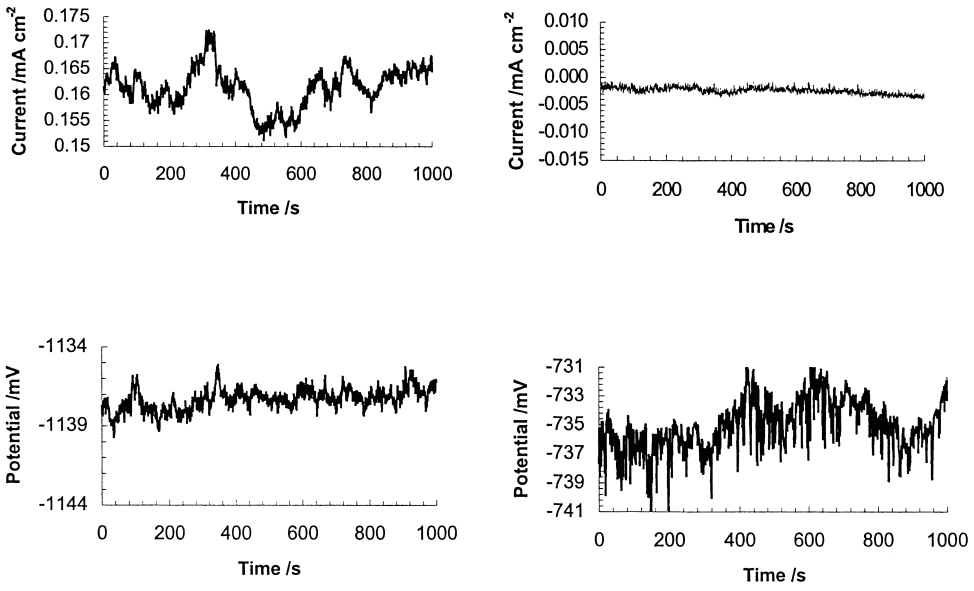

Fig. 1. Current and potential noise data recorded simultaneously for pure Al following 85-min immersion in a 0.005 mol dm^{-3} $In_2(SO_4)_3$ and 0.5 mol dm^{-3} NaCl solution (left) and in 0.5 mol dm^{-3} NaCl and 0.015 mol dm^{-3} Na_2SO_4 (right).

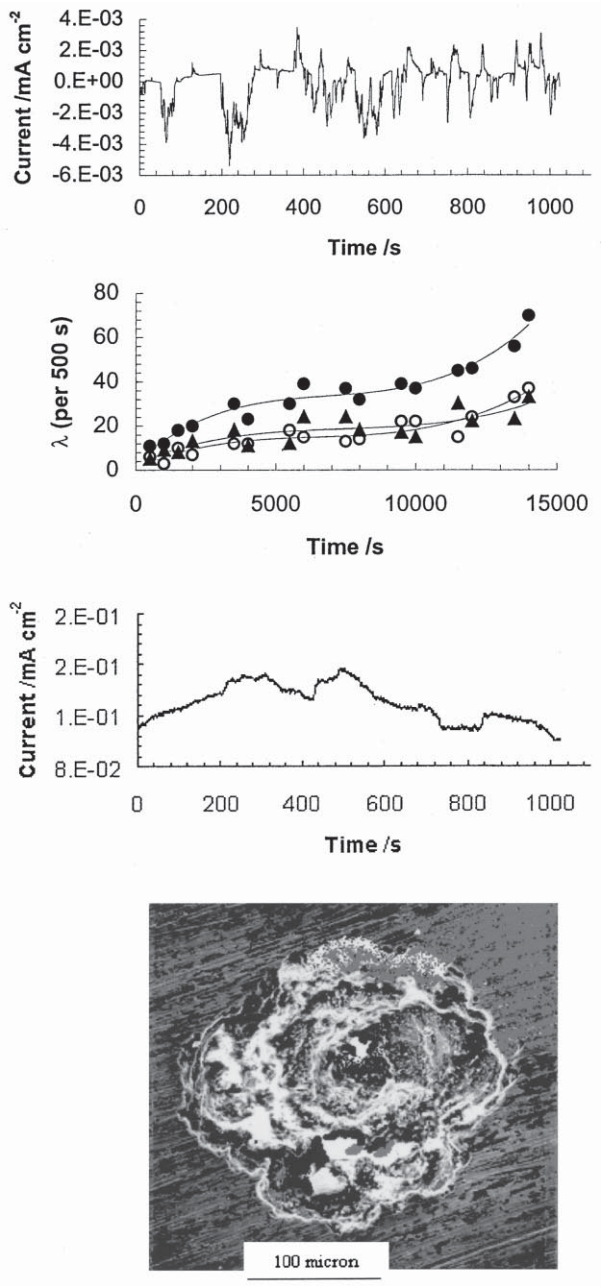

Fig. 2. (a) Current–noise plot recorded for aluminium in the absence of indium. (b) Pit nucleation frequency, λ, as a function of time for aluminium in the absence of indium. ●: Total number of pits nucleated, ○▲: number of pits nucleated on individual electrodes; (c) Current–noise plot recorded for aluminium in the presence of indium after 5-h immersion. (d) SEM micrograph following immersion in the indium-containing solution.

3. Results

In Fig. 1, current- and potential–time transients for aluminium immersed in the acidified chloride solution and in the chloride solution containing indium salt, are shown. These data were recorded following an 85-min immersion period in the test solutions. For comparative purposes, the current and potential axes are chosen so as to span 0.025 mA and 10 mV, respectively. It is evident from these time records that the presence of indium in solution accelerates the dissolution of aluminium and a much larger current and more electronegative potentials are recorded. Also, much larger current fluctuations and less pronounced potential fluctuations are recorded for aluminium in the indium-containing solution. The mean current recorded in the acidified chloride solution is close to 0 and fluctuates from positive to negative values, indicating that both electrodes are indeed similar. However, the current–time data recorded in the indium-containing solution indicate the preferential dissolution of one electrode only.

In the case of aluminium electrode immersed in the chloride solution, but to a lesser extent, in the indium-containing solution, it was possible to differentiate between individual pits. This can be seen from the data presented in Fig. 2(a), where the current-time transients are shown for aluminium in the chloride solution. These data were recorded once the measured electrode potential reached −0.730 V(SCE), which is the pitting potential of aluminium in this solution. The baseline current is close to zero. Current fluctuations in the negative direction indicate the onset of meta-stable pitting attack at one electrode, while the current fluctuations in the positive direction indicate the onset of attack at the other electrode. The number of current fluctuations in successive 500-s intervals were counted for each of the electrodes and then expressed as a function of time. This plot can be seen in Fig. 2(b), where the frequency of pit nucleation is shown as a function of time for both electrodes and each individual electrode. It can be seen that the frequency of pit nucleation increases with time and that pit nucleation occurs at approximately the same rate for both electrodes. This type of behaviour was evident only in the very early stages of immersion for aluminium in the indium-containing solution. The potential adopted by the electrodes during this time was about −1.137 V(SCE), which is the breakdown potential of aluminium in an indium-containing electrolyte. The frequency of pit nucleation exceeded 55 events per 500 s during the first 500 s of immersion, but after that time it became impossible to determine the number of individual meta-stable pitting events. Indeed, after a few hours of immersion, general-like dissolution became evident, Fig. 2(c). The degree of localized attack on aluminium following immersion in the indium-containing solution is evident from the micrograph shown in Fig. 2(d). Here, a single pit site is shown. The white regions indicate the presence of indium, which is seen in high concentrations in the pit interior. The regions surrounding the pit remain passive and essentially free of deposited indium.

It is evident from Fig. 2(a) that the current increases as a function of time to reach a maximum value, I_{peak}, and then decreases to the baseline, as a meta-stable pitting event takes place. Peak currents, I_{peak}, were calculated for aluminium

immersed in the indium-containing solution and the chloride solution. These values were calculated by measuring the maximum current during the meta-stable pitting event and then subtracting from this value the baseline current, before the onset of the meta-stable pitting event. These data are shown in terms of cumulative probability plots in Fig. 3. Here, it can be seen that the peak currents are considerably higher in the indium-containing electrolyte. I_{peak} values in the chloride-containing solution fall below 2.5 μA, but can reach values as high as 10 μA in the indium-containing solution.

Another parameter that is used frequently in the study of pit propagation is the pit growth time t_g [11]. The pit growth period, t_g is defined as the time period between the onset or nucleation, of the pit and the point where the current reaches the maximum value I_{peak}. In Fig. 3(b) t_g values are shown in terms of

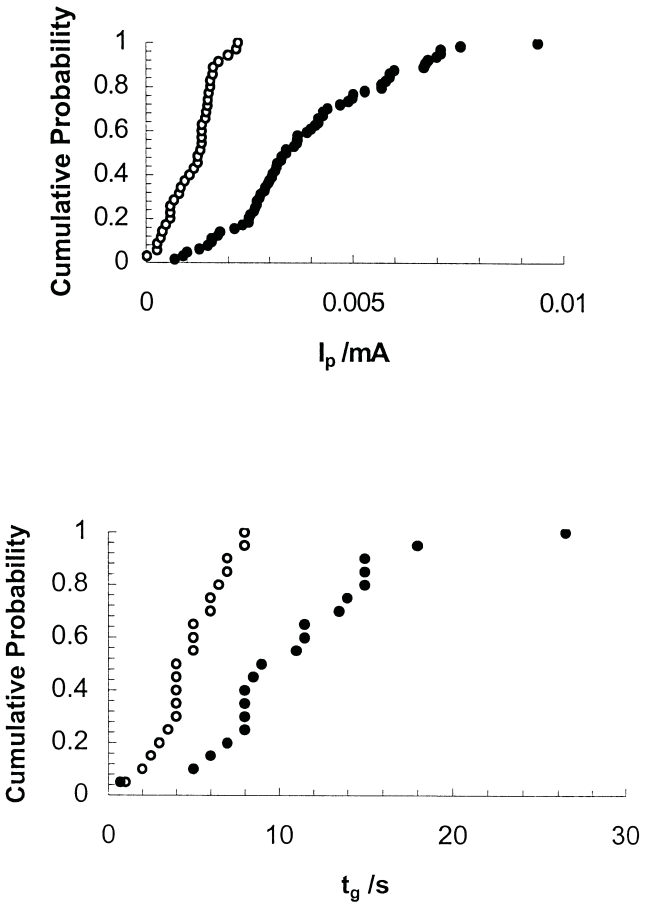

Fig. 3. Cumulative probability plots of: (a) peak current values I_{peak} and (b) pit growth times, t_g for aluminium in the: ● presence and ○ absence of indium.

cumulative probability plots for aluminium immersed in solution in the presence and absence of indium. Here, it can be seen that the average pit growth time in the absence of indium is about 5 s, while that in the presence of indium is approximately 10 s, with some pit growth times as high as 25 s. The pit growth rate, averaged over the time period t_g, was calculated as $(4.5 \pm 0.2) \times 10^{-3}$ mA s^{-1} in the absence of indium, but $(4.0 \pm 0.2) \times 10^{-3}$ mA s^{-1} in the presence of indium.

It was possible to obtain additional information from such time records by extracting from the records current–time data for the propagation of a single pit. For this purpose, the data were collected at a rate of 50 points per second and only the data measured during the very early stages of pit nucleation were used. The current–time transients were examined carefully and only those fluctuations which showed a clear current increase during the early stages were used, in order to ensure that only transients relating to single pits were analysed. This procedure was followed also to ensure that the data used did not involve contributions from pit repassivation. In this case, the current measured at a particular time, t, is proportional to the rate of pit propagation and concentration of dissolved aluminium from the active pit, which in turn are related to the dimensions or volume of the pit. Thus,

$$I_t = I_o + \alpha\big((\text{pit volume})_t\big) \tag{1}$$

$$I_\infty = I_o + \alpha\big((\text{pit volume})_f\big) \tag{2}$$

where I_t is the pitting current at time t and I_o is the original passive current before the onset of a pit, I_∞ is the pitting current at infinite time, pit volumes with subscripts f and t refer to the final pit volume, at infinite time, and the extent of pit development after time t, and α is a constant. Combining Eqs. (1) and (2) and assuming that this is a first-order process gives,

$$I_t - \big(I_\infty - \alpha\big((\text{pit volume})_f\big)\big) = \alpha\big((\text{pit volume})_t\big) = \alpha\big((\text{pit volume})_f\big)\, e^{-{}_1kt} \tag{3}$$

The use of the pitting current at infinite time and the final pit volume can be avoided by making use of pairs of observations, i.e. I_t and $I_{t+\Delta t}$. Thus,

$$I_t = (I_\infty - K) + K\, e^{-{}_1kt} \tag{4}$$

where I_∞ and I_o are again the currents measured at final pit volume and before the onset of pitting and K is a constant, incorporating α and the infinite pit volume, and ${}_1k$ is the first-order rate constant. The value of I at a subsequent time, $t + \Delta t$, is given as

$$I_{t+\Delta t} = (I_\infty - K) + K\, e^{-{}_1kt}\, e^{-{}_1k\Delta t} \tag{5}$$

On subtraction of these two equations, one obtains the relationship,

$$I_{t+\Delta t} - I_t = K'\, e^{-{}_1kt} \tag{6}$$

where K' is a constant. In Fig. 4, representative plots of $\ln(I_{t+\Delta t} - I_t)$ as a function of time, in accordance with Eq. (6), are shown for the propagation of a pit on aluminium immersed in the indium-containing electrolyte. Only transients that exhibited a sharp rise in current during the early stages of propagation were used. In addition, only the current readings recorded during the early stages of pit development, where activation–repassivation events were apparently absent, were considered. Two representative plots recorded for aluminium immersed in the indium-containing solution are shown in Fig. 4. Similar data for activation of aluminium in the acidic chloride solution were obtained. It can be deduced from these data that the rate-determining step in pit propagation follows a pseudo first-order process. Pseudo first-order rate constants of $(7.6 \pm 1.3) \times 10^{-3}$ and $(4.1 \pm 1.2) \times 10^{-3}$ s^{-1} were calculated for aluminium in the presence and absence of indium. This suggests that the rate of pit propagation, during the very early stages of propagation, is approximately two times higher in the presence of indium in solution.

In Fig. 5(a) and (b), power spectrum density plots are shown for aluminium in the presence and absence of indium, respectively. The average potential in the case of the indium-containing system was −1138 mV(SCE), while that measured in the absence of indium was −810 mV(SCE). Also in this figure, the spectral noise impedance, which is calculated as,

$$R_{sn}(f) = \left| \frac{V_{fft}(f)}{I_{fft}(f)} \right|^{1/2} \tag{7}$$

is shown.

The power spectrum density plots exhibit a $1/f^n$ trend in the high-frequency region. A low frequency plateau, which occurs at a cut-off frequency of about 0.01 Hz, is evident in the potential PSD plot, when indium in present in the electrolyte. However, this is not evident for the chloride solution, Fig. 5(b). The current noise

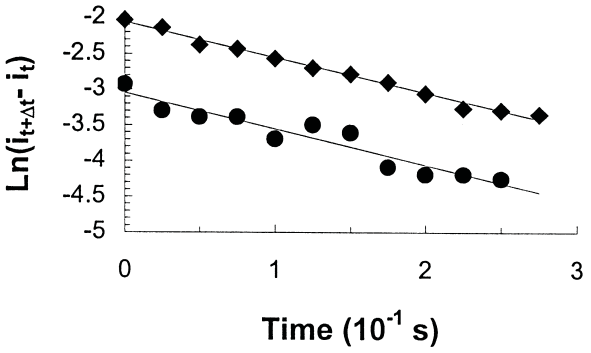

Fig. 4. A plot of the logarithm of $(I_{t+\Delta t} - I_t)$ as a function of time (left) and the corresponding current–time relationship (right) for the formation of a pit on pure aluminium in the presence of indium.

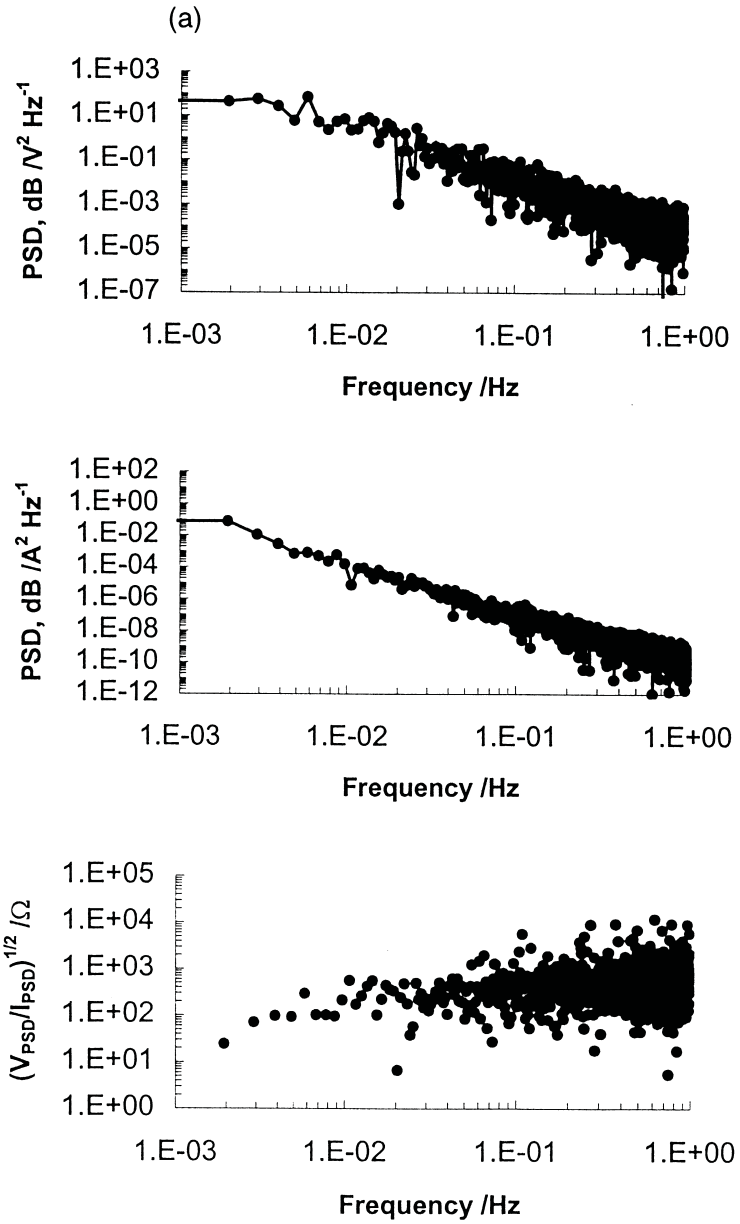

Fig. 5. Power Spectral density plots of (top) potential (centre) current and (bottom) ratio, $(V_{psd}/I_{psd})^{1/2}$, for (a) Al in the presence of indium and (b) Al in the absence of indium.

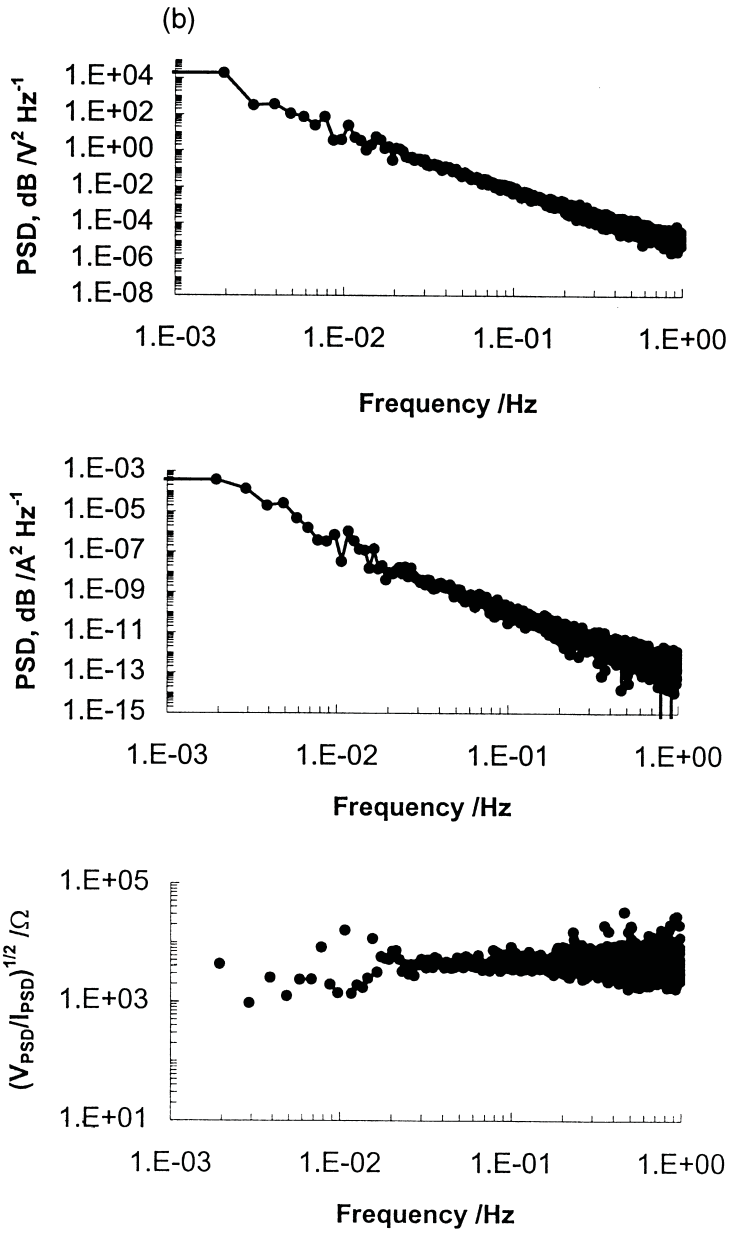

Fig. 5 (*continued*)

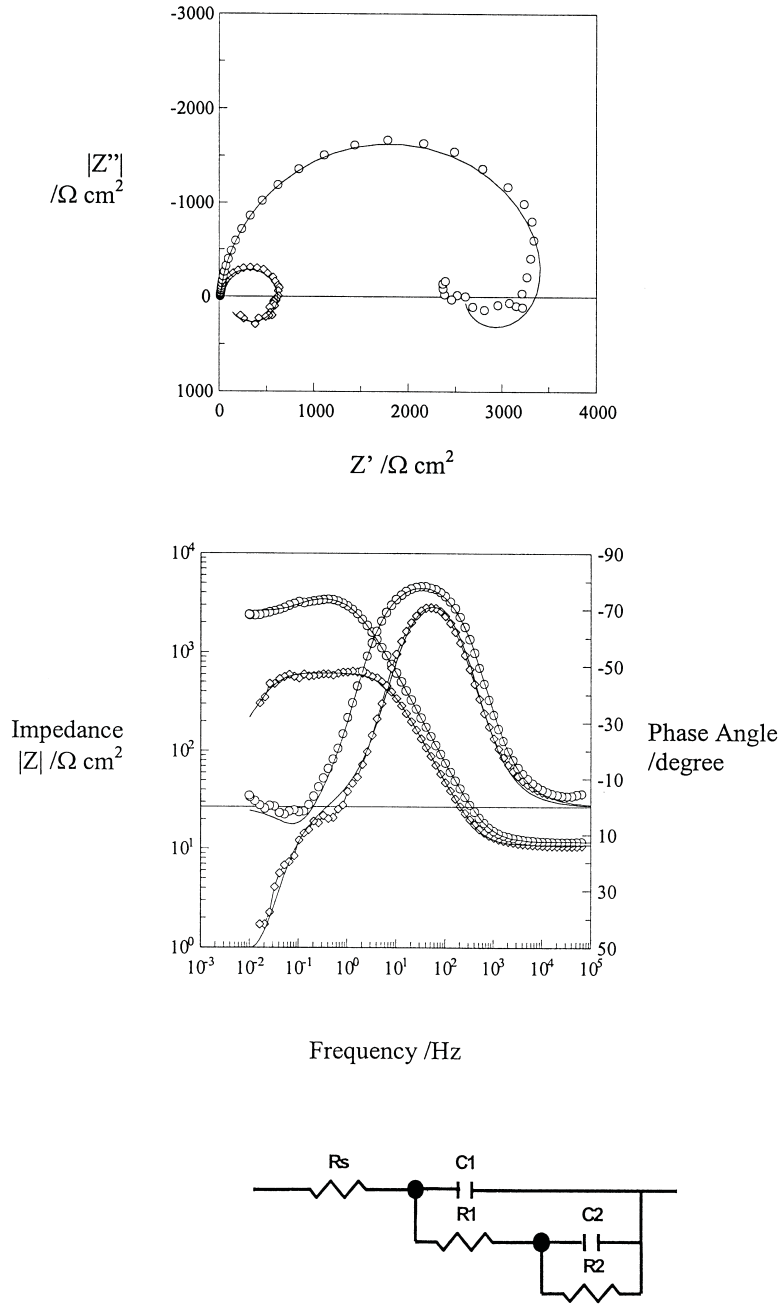

Fig. 6. Impedance data recorded for Al in: ◇ the absence of indium, ○ the presence of indium. Bode plot, Nyquist plot and equivalent circuit. Simulated spectra shown as solid lines.

level is considerably higher in the case of the indium-containing system, approximately a factor of 10^2 greater than that observed in the chloride-containing solution. This is consistent with the higher dissolution rates observed in the indium-containing solution, and the large fluctuations observed in Fig. 1. The potential noise level is however considerably lower for the electrode immersed in the indium-containing solution, but again this is consistent with the time records, Fig. 1, where a much 'noisier' potential is evident for the electrode immersed in the acidic chloride solution. It can be seen, from the spectral noise impedance plots, that the spectral noise impedance is higher for the electrode immersed in the acidic chloride solution. Also, the spectral noise impedance is essentially independent of frequency in the case of the chloride solution, but exhibits decreasing impedance at low frequencies in the case of indium-containing solution.

Impedance data, recorded for aluminium in the chloride solution and chloride solution containing indium, are shown in Fig. 6(a), where Bode plots and Nyquist diagrams are presented. These impedance data were recorded after 240 min of immersion (in order to approach stationary conditions), under open-circuit conditions, where the open-circuit potentials were −1135 and −810 mV(SCE) in the presence and absence of indium, respectively. These potentials were chosen so that the measurements were carried out under conditions as close as possible to those existing in the case of noise measurements. These spectra exhibit a high frequency capacitive region and a lower frequency inductive region. These data were fit to the equivalent circuit shown in Fig. 6(b). The circuit is based on a model used by Franceschetti and Macdonald [23], Armstrong [24] and Pettersson and Pound [25] to model systems involving passivation or adsorption-type reactions. A negative resistance, R_2, and capacitance C_2 are used to model the inductive behaviour as opposed to using very high inductances. The other parameters in the circuit, R_1 and R_2 are resistance elements, where R_1 is the solution resistance, while Q_1 is a constant-phase element. The impedance of a constant-phase element, is defined as $Z_{\mathrm{CPE}} = [Q(j\omega)^n]^{-1}$ where $-1 \leq n \leq 1$ [26]. The n value was close to unity in the case of Q_1 indicating that Q_1 is a true capacitance element. Both, the experimental and simulated data are shown in Fig.

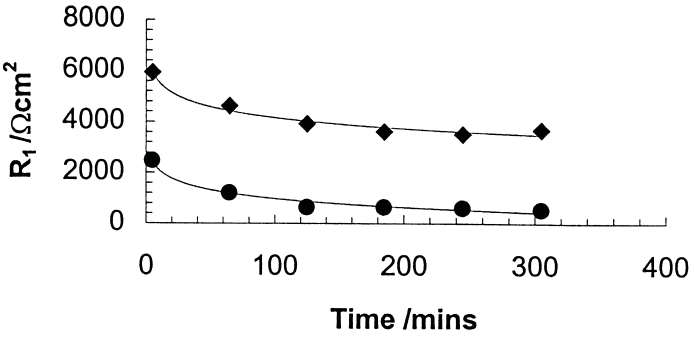

Fig. 7. R_1 plotted as a function of time for Al in: ◆ the absence of indium, ● the presence of indium.

6(a) illustrating that a good fit between the experimental and theoretical data was obtained. In Fig. 7, a plot of R_1 as a function of time for Al immersed in solution in the presence and absence of indium is shown. Here, it can be seen that R_1 is reduced almost by an order of magnitude in the presence of indium. This is consistent with the higher dissolution rates induced by indium. The parameter, R_2, was almost a factor of two greater for aluminium immersed in the acidic chloride solution. The actual significance of this parameter is not clear, but it is consistent with the oxidation current being impeded by an inductive current flowing in the opposite direction at the electrode/electrolyte interface. This may be associated with the formation and precipitation of a salt film which can occur under these acidic conditions. This is supported by the fact that on slightly increasing the alkalinity of these solutions, this inductive loop disappears.

Very good agreement between the spectral noise impedance and the modulus of the impedance recorded using impedance spectroscopy was observed. Representative plots showing the spectral noise impedance and impedance for aluminium in the indium-containing solution are shown in Fig. 8. The impedance was recorded at the open-circuit potential, which was equal to the potential measured in the noise measurements. The decreasing impedance at low frequencies is evident in both measurements and the agreement between both sets of data is very good at all frequencies.

In Fig. 9, the parameters, R_1 and $R_1 - |R_2|$ calculated from the impedance data are compared to the values of R_{sn} calculated at a frequency of 1 mHz for aluminium in the presence and absence of indium. The values of R_1 are somewhat higher than the corresponding values of R_{sn}, but very good agreement is observed between the values of $R_1 - |R_2|$ and R_{sn}. Thus, the value of R_{sn} at 1 mHz, where the contributions of the component R_2 become clearly evident as in Fig. 7, represents contributions from R_1 and R_2. This is also clearly seen in Fig. 5.

The noise resistance parameter R_n, which is defined as the ratio of the standard deviation of the potential and current noise signals was evaluated as $(4.1 \pm 0.2) \times$

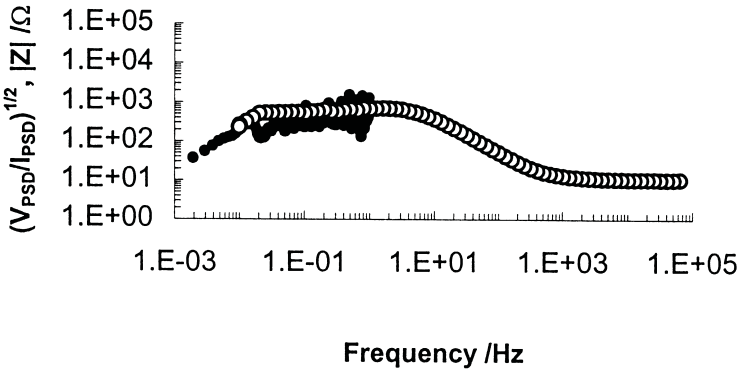

Fig. 8. ○: Impedance modulus $|Z|$ and ●: spectral noise resistance R_{sn} for Al in an indium-containing solution.

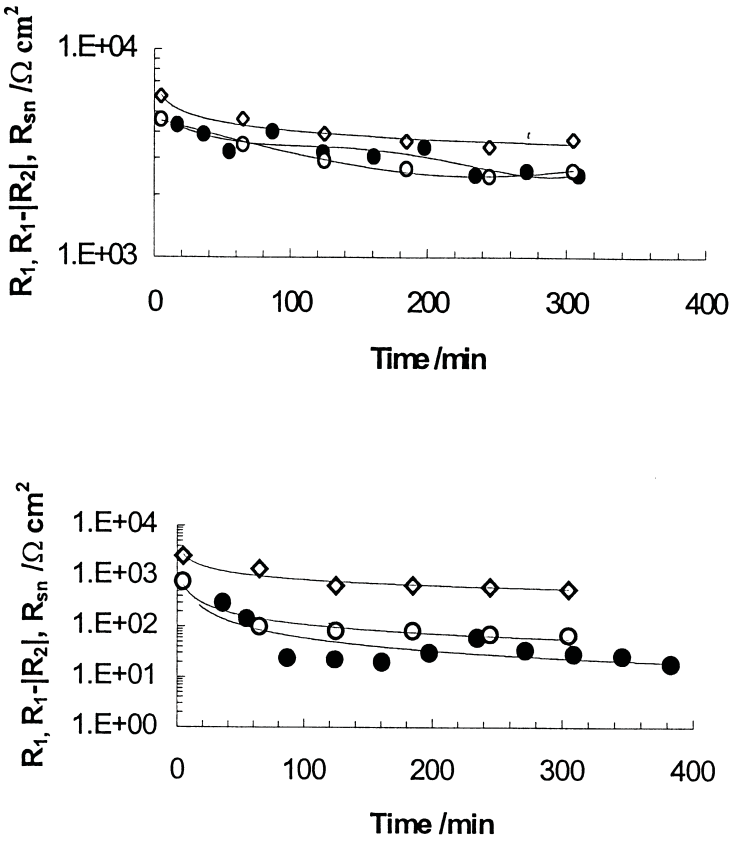

Fig. 9. ◇: R_1, ○: $R_1 - |R_2|$ line calculated from impedance data, and •: R_{sn} (at 1 mHz) calculated from noise data plotted as a function of time for Al in the absence of indium (top) and Al in the presence of indium (bottom).

$10^3\ \Omega\ cm^2$ for aluminium in the chloride solution and as $(7.5 \pm 0.5) \times 10^1 \Omega\ cm^2$ for aluminium in the indium-containing solution. These values were averaged over 15 different individual runs. The R_n value calculated in the case of the chloride solution is in close agreement with both, the electrochemical impedance data and the value of R_{sn} at 1 Hz, which is also close to the low frequency limits of $|Z|$ and R_{sn}, Figs. 7 and 9. The R_n value calculated in the indium-containing solution is somewhat lower than either the impedance, or the R_{sn} values calculated at 1 Hz, Figs. 7–9. However, the value is close to the low frequency limit of the impedance.

4. Discussion

The electrochemical noise data presented in this communication show clearly

that the presence of indium dissolved in solution exerts a considerable activating effect on aluminium, in agreement with previous studies [27]. It can be seen, also, that the electrochemical noise data provide useful information, in both, the time and frequency domains.

The analyses in the time domain show that the average pit growth rate, under freely corroding conditions, is comparable in the presence and absence of indium in the acidified chloride solution. However, based on the average pit growth times, Fig. 3(b), and visual examination of the specimens, significantly larger pits are formed in the presence of indium. It is seen, also, from the data presented in Fig. 4, that the initial pit propagation rate is higher in the presence of indium. These observations are consistent with the fact that indium is initially deposited, in relatively small quantities, at the surface, through an oxidation–reduction type reaction,

$$Al + In^{3+} \rightarrow In + Al^{3+}$$

Indeed, this was confirmed by energy dispersive X-ray analyses where precipitates of indium could be found on the electrode surface prior to activation [12,27]. The resultant Al–In surface alloy that is formed, facilitates the onset of local attack, with the initial rate of attack being approximately twice as high as that observed in the acidified chloride solution. As aluminium dissolves into the forming pit, a highly acidified pit solution, dissolution–repassivation events, and the possibility of a salt film reduces the rate of attack to a level comparable to that observed in the absence of indium. However, repassivation does not occur, as in the case of the acidified chloride solution, primarily because of the occurrence of an auto-catalytic type reaction, in which even greater amounts of indium are deposited within the developing pit, Fig. 2(d). This is consistent with the large amounts of indium detected in the interior of pits [12,27].

Good agreement between the spectral noise impedance, R_{sn}, and the impedance $|Z|$ was obtained in the presence and absence of indium, provided the impedance and the noise measurements were collected under similar potential conditions. Indeed, by estimating R_{sn} at 1 mHz, a reasonably good approximation of the charge transfer resistance, $R_1 - |R_2|$ can be obtained, Fig. 9. However, again, care had to be taken to ensure that the measurements were recorded under similar potential conditions. The open-circuit potentials recorded in the presence of indium were very reproducible from experiment to experiment. However, the open-circuit potentials recorded in the chloride solution varied from about -715 mV, where pitting attack occurs, to -870 mV, and also varied as a function of the immersion period. Similar observations were made by Bertocci et al. [16] for aluminium in 1 mol dm^{-3} KCl solution.

The magnitude of noise resistance R_n, which is calculated in the time domain approaches the low frequency limits of both R_{sn} and $|Z|$. Bertocci et al. [16] have shown that the relationship between R_n and $R_{sn}(f)$ is,

$$R_n(T) = \sqrt{\int_{f_{min}}^{f_{max}} \psi_V \, df / \int_{f_{min}}^{f_{max}} \psi_I \, df} \tag{8}$$

where T is the measurement time of each record used for calculating the PSD. If the R_{sn} or $|Z|$ spectra exhibit a low frequency plateau, then the right hand side of Eq. (8) returns a value corresponding to the zero frequency limit of $|Z|$. This is exactly the situation that exists in the present work, and thus it could be expected that good agreement between the R_n value processed in the time domain, and the zero frequency limit of $|Z|$ would be obtained.

5. Conclusion

Information on the rate of pit growth, under freely corroding conditions, in the presence and absence of indium in an acidified chloride solution was obtained from current noise measurements in the time domain. Comparable average pit-growth rates were obtained in the presence and absence of indium. However, pit growth times were considerably higher in the presence of indium. The initial breakdown process followed a pseudo first-order process. The rate constant for this pseudo first-order process was almost a factor of two greater in the case of indium-containing solution, indicative of a faster rate of initial breakdown in the presence of indium. Spectral noise plots, obtained on analysing the noise data in the frequency domain, agreed well with impedance spectra, measured under similar conditions. Good agreement was also obtained between R_n, processed in the time domain, and the zero frequency limit of the impedance. It can be seen from these data that the current–noise measurements provide much information and they show clearly that the presence of indium in solution activates aluminium, in agreement with previous publications.

Acknowledgements

The authors gratefully acknowledge the support of this work, in part, by Enterprise Ireland, under the Basic Science Research Grants Award, Project Code SC/96/456.

References

[1] J.T. Reding, J.J. Newport, Mater. Protection 5 (1966) 15.
[2] A.R. Despic, D.M. Drazic, M.M. Purenovic, N. Cikovic, J. Appl. Electrochem 6 (1976) 527.
[3] Y. Hori, J. Takao, H. Shomon, Electrochim. Acta 30 (1985) 1121.
[4] C.D.S. Tuck, J.A. Hunter, G.M. Scamans, J. Electrochem. Soc 134 (1987) 2070.
[5] M.C. Reboul, P. Gimenez, J.J. Rameau, Corrosion 40 (1984) 366.
[6] A. Mance, D. Cerovic, A. Mihajlovic, J. Applied Electrochem 15 (1985) 415.
[7] G. Burri, W. Leudi, O. Haas, J. Electrochem. Soc 136 (1989) 2167.

[8] A. Mihajlovic, A. Mance, O. Nesic, J. Serb. Chem. Soc 52 (1987) 663.
[9] J. Hunter, G. Scamans, J. Sykes, Power Sources 13 (1991) 193.
[10] C.B. Breslin, W.M. Carroll, Corros. Sci 33 (1992) 1735.
[11] F. Sato, R.C. Newman, Corrosion 54 (1998) 955.
[12] W.M. Carroll, C.B. Breslin, Corros. Sci 33 (1992) 1161.
[13] K. Hladky, J.L. Dawson, Corros. Sci 21 (1980) 317.
[14] P.C. Searson, J.L. Dawson, J. Electrochem. Soc 135 (1988) 1908.
[15] F. Mansfeld, H. Xiao, J. Electrochem. Soc 140 (1993) 2205.
[16] U. Bertocci, C. Gabrielli, F. Heut, M. Keddam, P. Rousseau, J. Electrochem. Soc 144 (1997) 37.
[17] C. Monticelli, F. Zucchi, F. Bonollo, G. Brunoro, A. Frignani, G. Trabanelli, J. Electrochem. Soc 142 (1995) 405.
[18] C.T. Chen, B.S. Skerry, Corrosion 47 (1991) 598.
[19] B.S. Skerry, D.A. Eden, Prog. Org. Coat 15 (1987) 269.
[20] U. Bertocci, C. Gabrielli, F. Heut, M. Keddam, J. Electrochem. Soc 144 (1997) 31.
[21] H. Xiao, F. Mansfeld, J. Electrochem. Soc 141 (1994) 2332.
[22] F. Mansfeld, L.T. Han, C.C. Lee, J. Electrochem. Soc 143 (1996) L286.
[23] J.R. Macdonald, Impedance Spectroscopy, Wiley, New York, 1987.
[24] D.R. Franceschetti, J.R. Macdonald, J. Electroanal. Chem 82 (1977) 271.
[25] D. Armstrong, J. Electroanal. Chem 34 (1972) 387.
[26] R.F.A. Jargelius-Pettersson, B.G. Pound, J. Electrochem. Soc 145 (1998) 1462.
[27] C.B. Breslin, L.P. Friery, Corros. Sci 36 (1994) 231.